Fig. S1

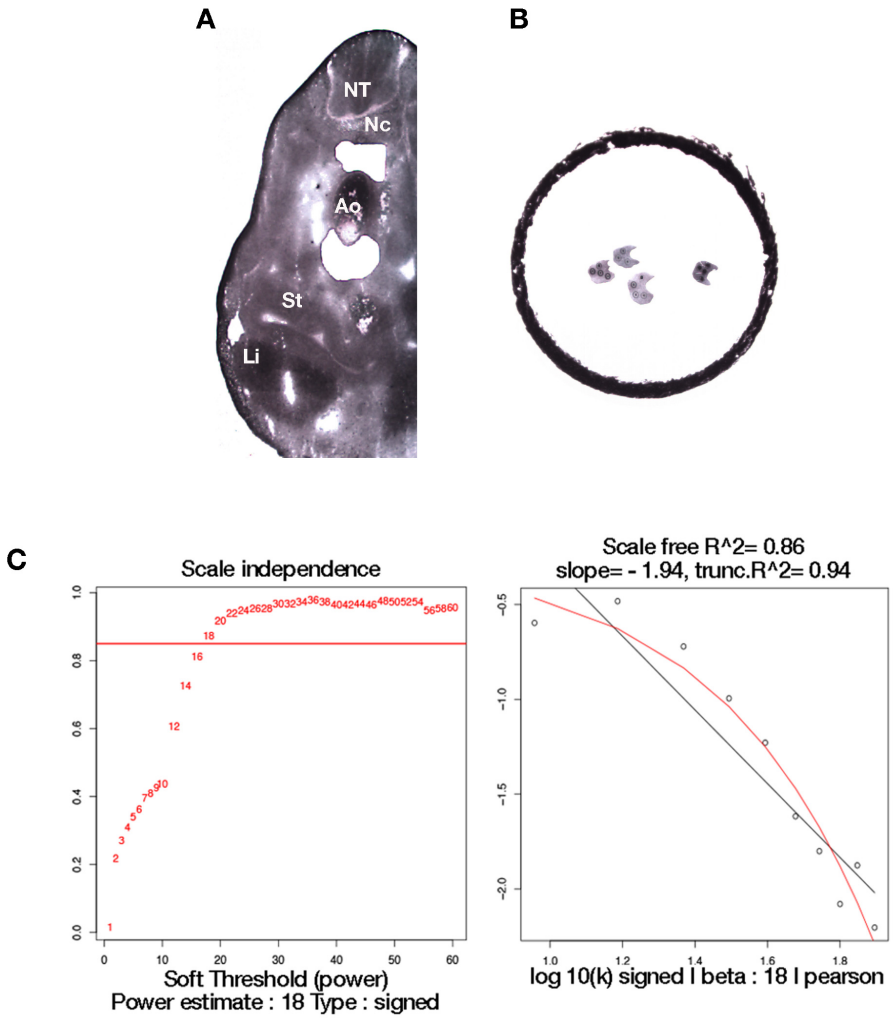

Fig. S1. Laser microdissection and WGCNA parameters (Related to Figures 1 and 2). (A) Laser microdissection. Representative image after laser microdissection on E11.5 section. The white areas above and below the dorsal aorta show the dorsal and ventral micro-dissected tissues, respectively. NT: neural tube; Nc: notochord; Ao: dorsal aorta; St: Stomach and Li: liver.

(B) Representative image of E11.5 micro-dissected ventral aortic tissues collected on a specific cap for RNA extraction.

(C) WGCNA selection parameters. Left panel: Plot for choosing the power ß of the signed weighted correlation networks; the square of the correlation coefficient between the connectivity frequency and the binned connectivity is represented on the y-axis, while the different powers adjusting the adjacencies are given on the x-axis. Right panel: Connectivity distribution using ß power of 18. The black straight line corresponds to a power law fit and the red line to an exponentially truncated power law one.

Fig. S2

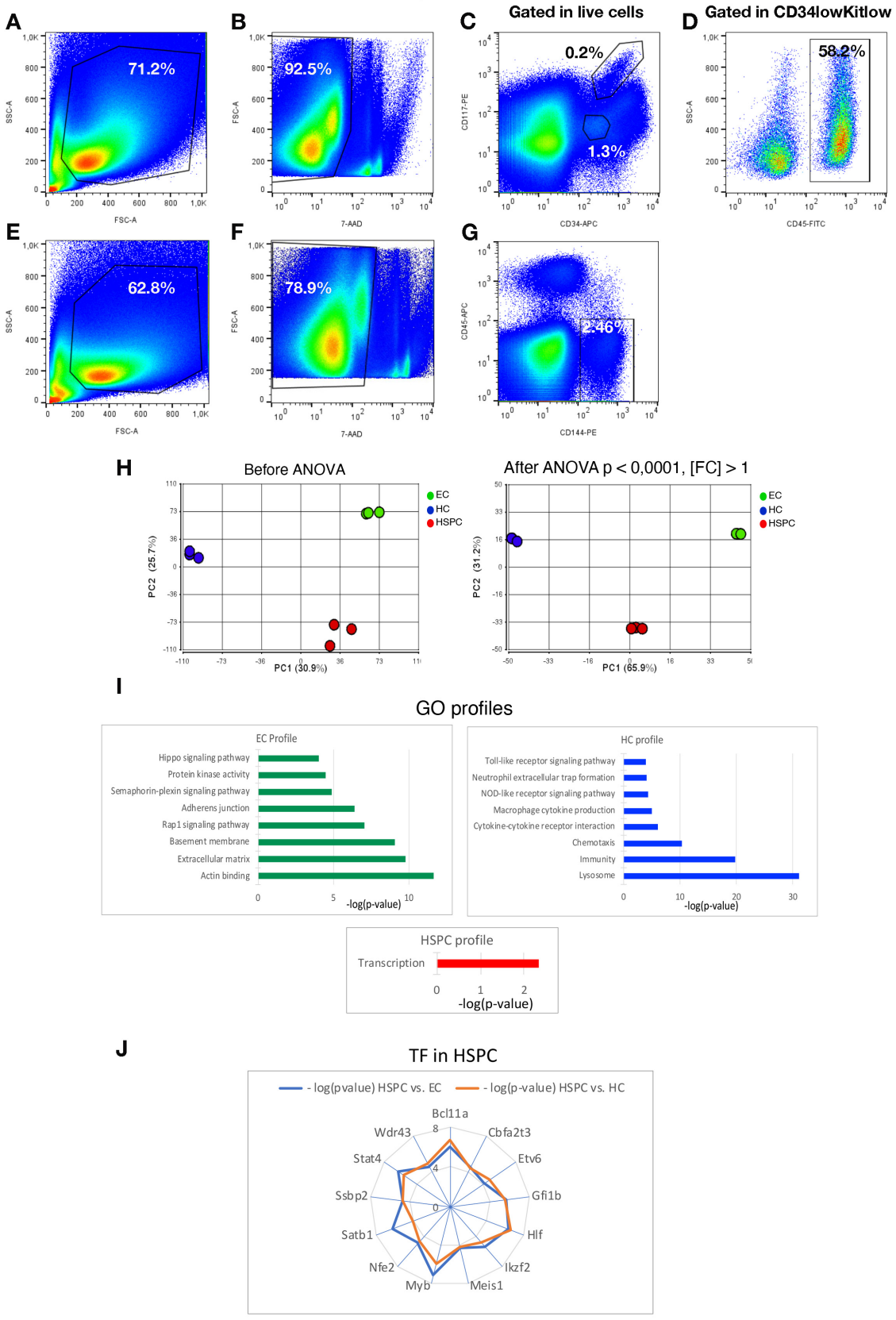

Fig. S2. Gating strategies and transcriptomics analyses of E11.5 AGM endothelial, hematopoietic and HSPC cell fractions (Related to Figure 2).

(A-G) Flow cytometry plots illustrating the strategies for isolating $CD34^{high}ckit^{high}$ HSPCs, $CD34^{low}ckit^{low}CD45^{+}$ hematopoietic cells (A-D) and $CD144^{+}CD45^{-}$endothelial cells (E-G).

(H) PCA before and after ANOVA.

(I) Gene ontology on the differentially expressed genes in endothelial cells (EC), hematopoietic cells (HC) and HSPCs.

(J) Genes encoding transcription factors differentially expressed in HSPCs as compared to ECs and HCs.

Fig. S3

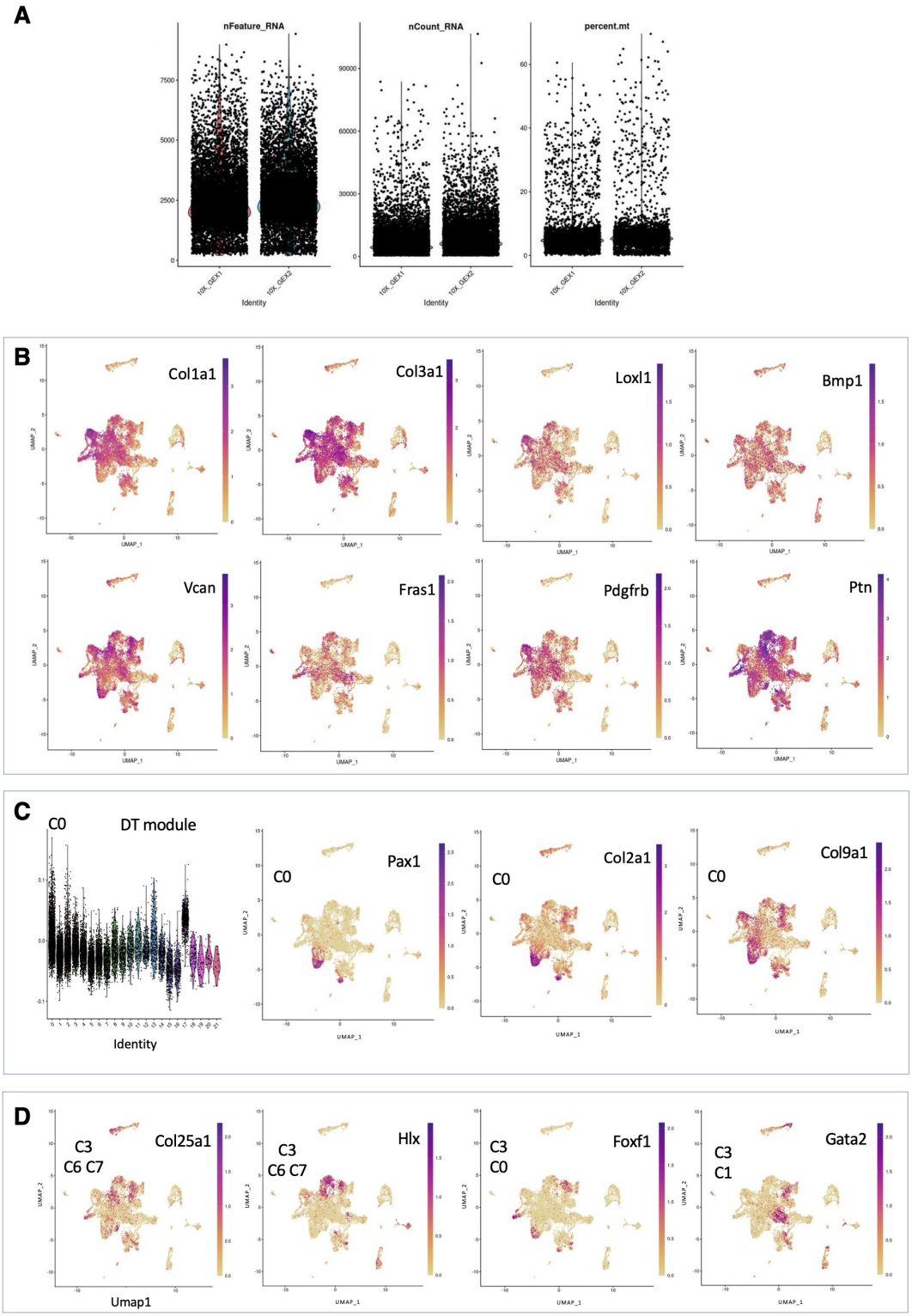

Fig. S3. Quality controls for single cell RNAseq and UMAP expression patterns (Related to Figure 3).

(A) scRNAseq Quality Control: Violin plots showing the number of genes, transcripts and percentage of mitochondrial RNA detected in each scRNAseq sample before filtering.

(B) UMAP expression pattern of genes defining the mesenchymal cell population.

(C) Distribution of genes of the DT 'turquoise' WGCNA module among the different clusters. Extreme left panel: projection of the DT module genes onto the - Louvain clusters; most genes project onto the C0 cluster. Other three panels: example of UMAP expression patterns of genes of the DT 'turquoise' WGCNA module.

(D) UMAP expression of genes the C3 cluster of the mesenchymal population.

Fig. S4

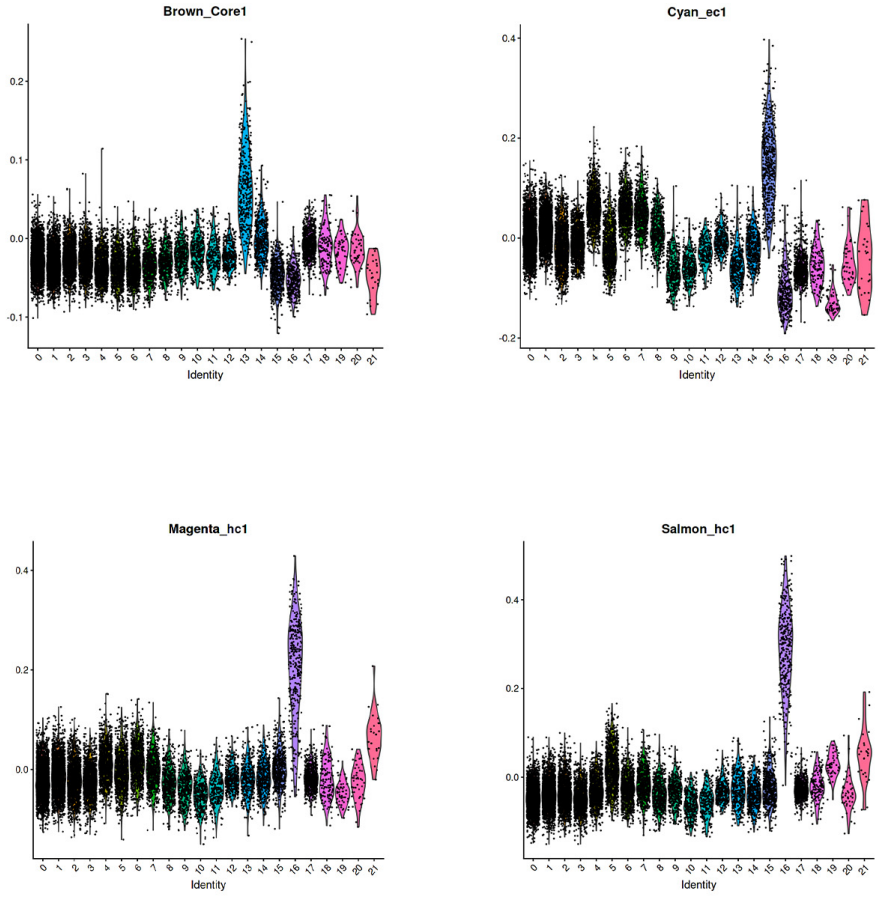

Fig. S4. Violin plots (Related to Fig. 3).

Violin plots showing the projection of genes of WGCNA modules into the single cell E11.5 AGM expression map.

Fig. S5

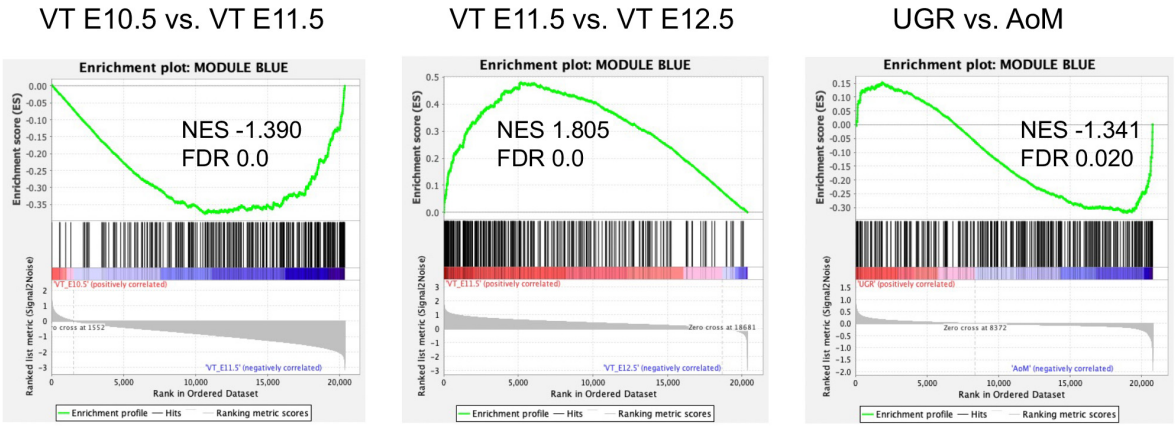

Fig. S5. Gene Set Enrichment Analysis (Related to Fig. 4).

The WGCNA 'blue' module is used as a gene set of reference to interrogate the global transcriptomes of ventral tissues at E10.5, E11.5 and E12.5, and of AGM stromal lines.

Fig.S6

CS14/4w

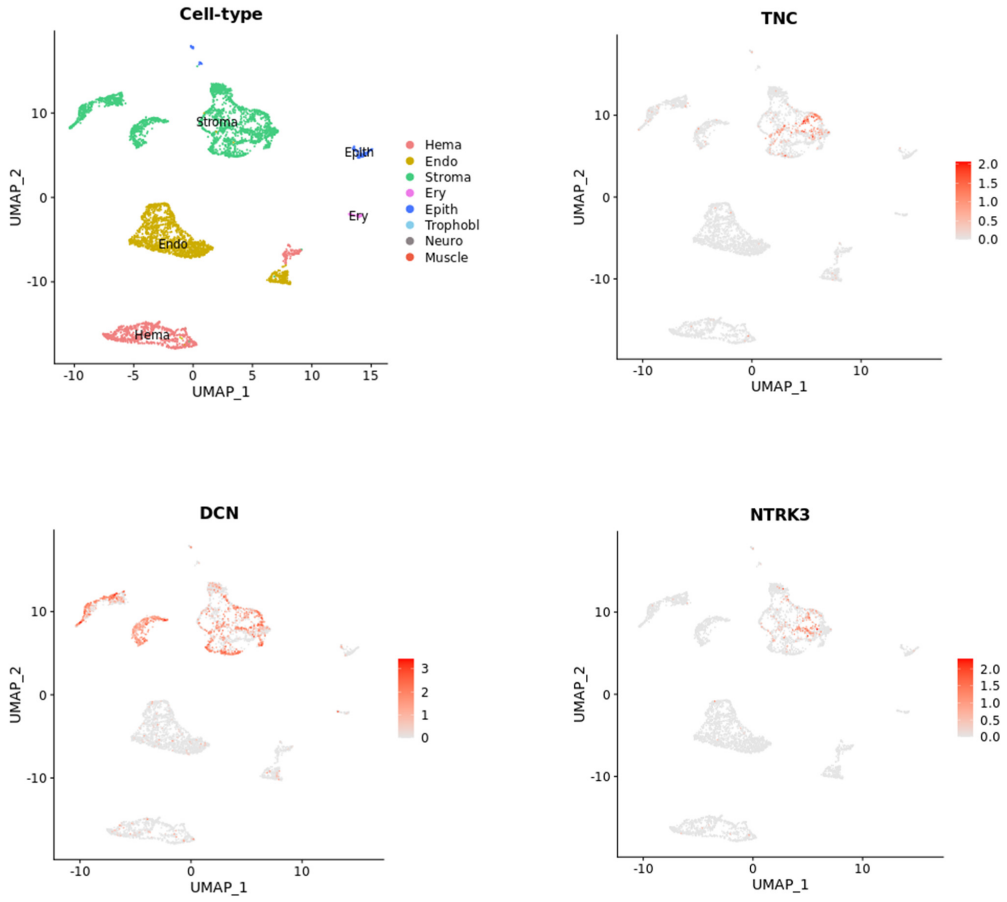

Fig. S6. Expression profiles of candidate genes in the embryonic human transcriptomics atlas (Related to Fig. 5).

Expression profiles of TNC, DCN and NTRK3 in the single cell embryonic human atlas at Carnegie Stage (CS) 14, corresponding to 4 weeks (4w) (Calvanese et al, 2022).

Fig. S7

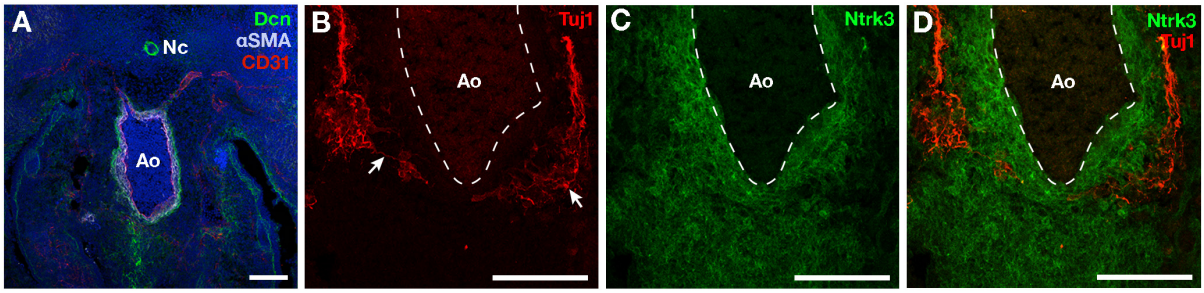

Fig. S7. Immunodetection for Dcn, Tuj1 and Ntrk3 on E11.5 mouse embryonic sections (Related to Fig. 5).

(A) Immunodetection of Dcn, CD31 and αSMA.

(B-D) Immunodetection of Tuj1 and Ntrk3. (D) represents the merge between Tuj1 and Ntrk3 staining. The dashed white line indicates the lumen of the dorsal aorta.

Scale bars: 100 μm.

Fig. S8

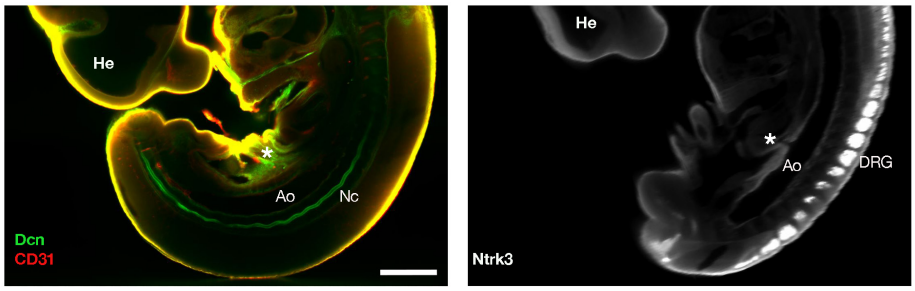

Fig. S8. Sagittal images from 3D imaging of E11.5 mouse embryos (Related to Fig. 5). Left, Dcn and CD31 staining; right, Ntrk3 staining. Nc: notochord, Ao: dorsal aorta, He: head, DRG: dorsal root ganglion. Scale bar: 0.75 mm.

Fig. S9

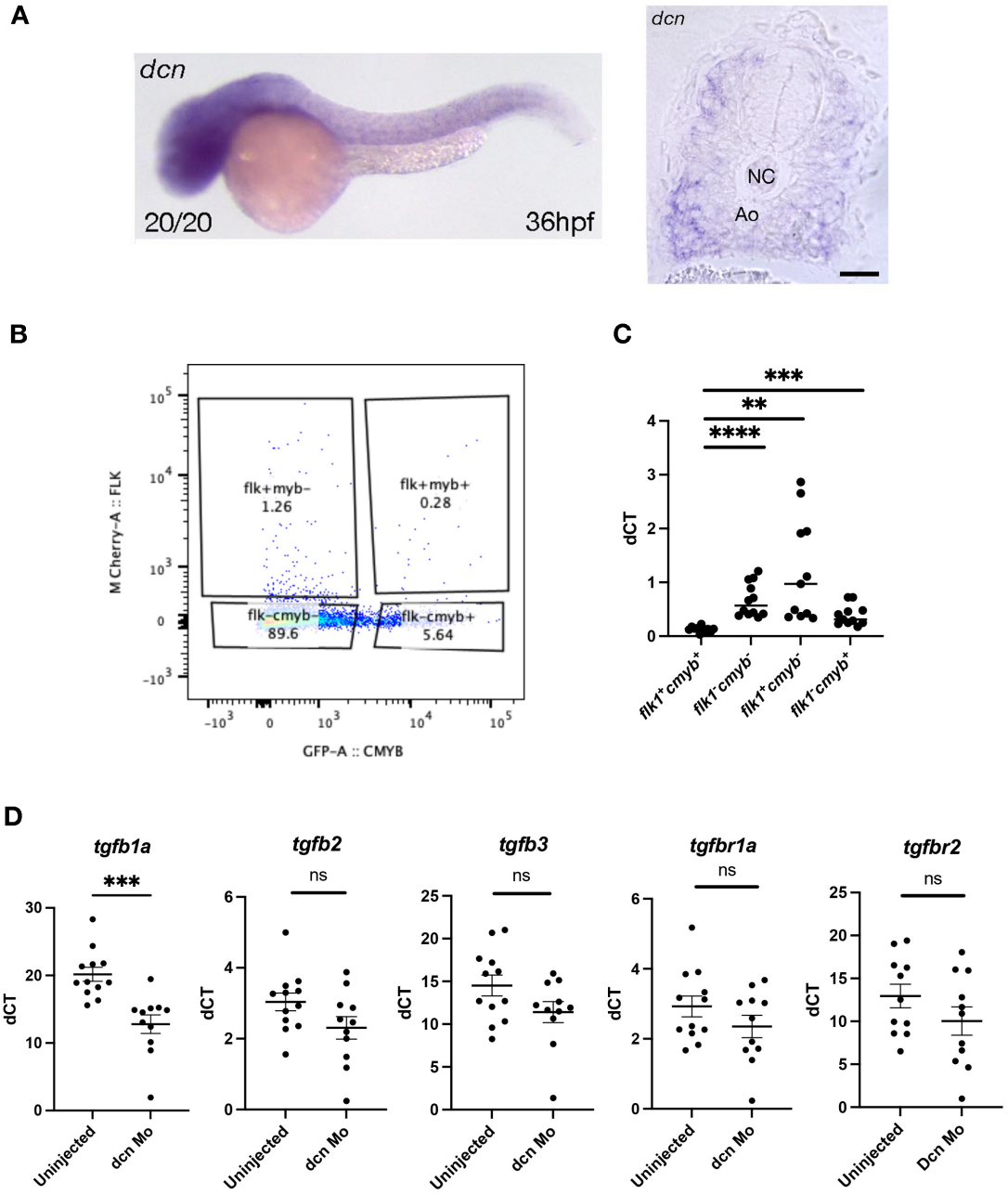

Fig. S9. *dcn* expression in zebrafish embryos and levels of tgfb signaling (Related to Figure 7).

(A) WISH for *dcn* in 36 hpf embryos. The numbers of embryos exhibiting the phenotype out of total is indicated in the left bottom corner. Image on the right shows *dcn* expression on a transverse section through the trunk of the embryo. Scale bar is 25 µm.

(B) Gating strategy to isolate *flk1*$^{-}$*cmyb*$^{-}$ *(*non-hematopoietic non-endothelial mesenchymal cells), *flk1*$^{-}$*cmyb*$^{+}$ (myeloid progenitors), *flk1*$^{+}$*cmyb*$^{-}$, (vascular endothelial cells) and *flk1*$^{+}$*cmyb*$^{+}$ (HSPCs) from the trunk of 48 hpf embryos using the *Tg(kdrl:mcherry;cmyb:gfp)* zebrafish line.

(C) RT-qPCR for *dcn* expression in the different cell fractions. N=4 experiments, two biological replicates and three technical triplicates for each experiment.
(D) RT-qPCR for *tgfb* pathway expression in uninjected and *dcn* MO^{START} morphants. N=4 experiments, four biological replicates run in three technical replicates. **** indicates $p<0.0001$, *** indicates $p<0.001$, ** indicates $p<0.01$ using unpaired t-test. ns indicates not statistically significant.

Fig. S10

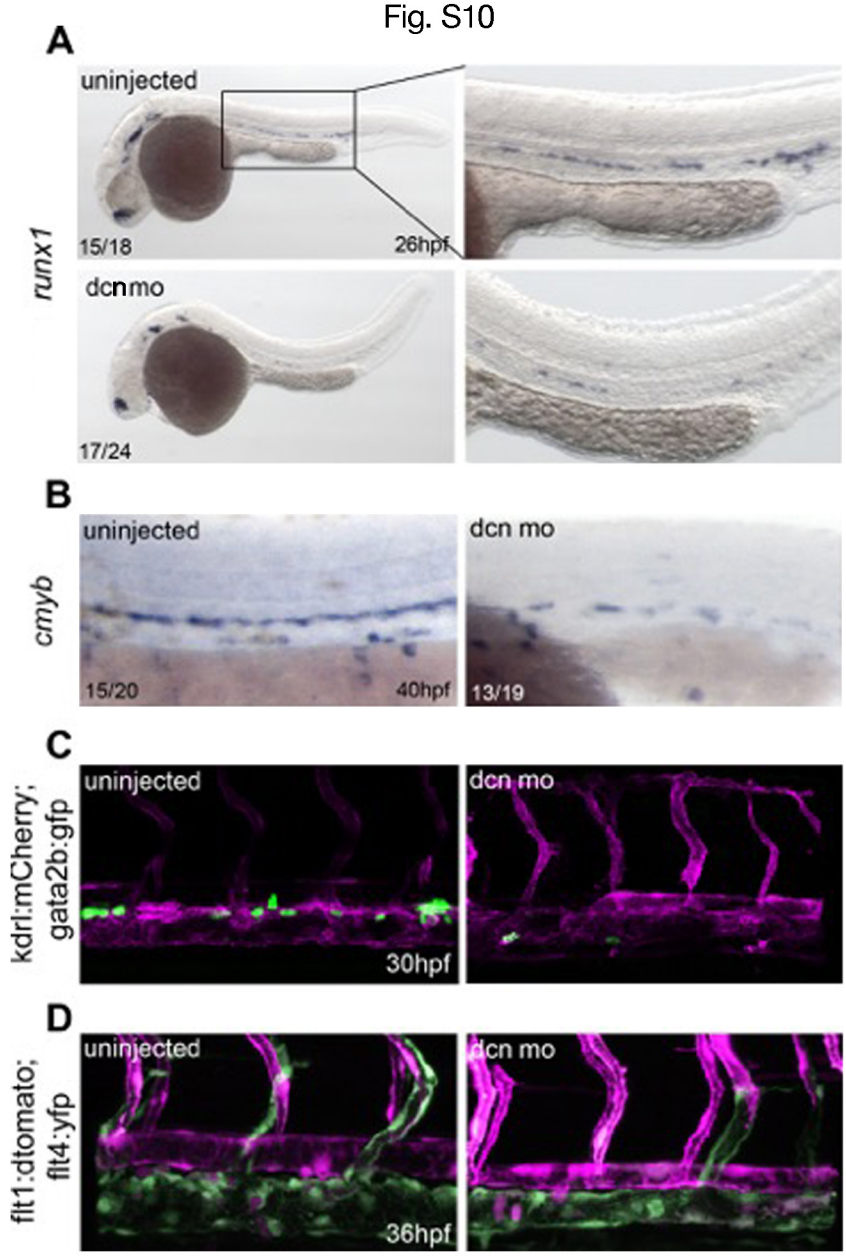

Fig. S10. Validation of the loss-of-function *dcn* phenotype (Related to Figure 7).

(A) WISH for *runx1* in 26 hpf *dcn* morphants embryos (MO^{SPLICE}) and their respective uninjected controls. Numbers of embryos with or without (out of total) *runx1* staining are indicated in the bottom left corner.

(B) WISH for *cmyb* in 40 hpf *dcn* morphants embryos (MO^{SPLICE}) and their respective uninjected controls. Numbers of embryos with or without (out of total) *cmyb* staining are indicated in the bottom left corner.

(C) Fluorescent microscopy of *kdlr:mCherry; gata2b :gfp* in 30 hpf *dcn* morphants embryos (MO^{SPLICE}) and their respective controls.

(D) Fluorescent microscopy of *flt1:dtomato; flt4:yfp* in 36 hpf *dcn* morphants embryos (MO^{SPLICE}) and their respective controls.

Fig. S11

Fig. S11. Loss-of-function experiments for *gdf6a* in zebrafish embryos (Related to Fig. 7).

(A-B) WISH for *runx1* in 30 hpf *gdf6a* morphants and their respective uninjected controls. (C) Numbers of *runx1*$^{+}$ cells in the dorsal aorta of control and *gdf6a* morphant embryos. Arrowheads indicate aortic HSPCs in the dorsal aorta. Data are from 3 independent experiments with 43 and 52 embryos for control and knock-down conditions, respectively. **** indicates $p<0.0001$ using a two-tailed unpaired t-test and Mann-Whitney test. Data are mean±s.e.m.

Table S1. Laser microdissection quantification at E10.5, E11.5 and E12.5.

This table indicates for each developmental stage the numbers of biological samples for VT and DT, the numbers of micro-dissected tissues, their corresponding surfaces and RNA concentrations.

Stage	Sample	Number of micro-dissected tissues	Total surface (µm2)	Amount of RNA (pg/µl)
E10.5	VT1	8	181917	100
E10.5	VT2	8	123901	336
E10.5	VT3	6	84431	120
E10.5	VT4	5	87885	45
E10.5	DT1	8	227741	182
E10.5	DT2	8	102109	91
E10.5	DT3	6	94265	93
E10.5	DT4	5	110030	23
E11.5	VT1	5	112256	256
E11.5	VT2	5	208447	581
E11.5	VT3	4	316542	294
E11.5	DT1	5	196256	420
E11.5	DT2	5	201851	334
E11.5	DT3	4	295497	581
E12.5	VT2	3	167725	310
E12.5	VT3	6	276511	29
E12.5	VT4	6	367767	125
E12.5	VT5	5	235330	59
E12.5	DT2	3	311436	822
E12.5	DT3	6	412076	324
E12.5	DT4	6	311614	126
E12.5	DT5	5	215926	239

Available for download at
https://journals.biologists.com/dev/article-lookup/doi/10.1242/dev.202614#supplementary-data

Table S2. The gene set accounting for the contrast between DT and VT tissues and the gene allocation to the different WGCNA modules.

Available for download at
https://journals.biologists.com/dev/article-lookup/doi/10.1242/dev.202614#supplementary-data

Table S3. Lists of genes within the blue WGCNA module with mesenchymal and neuronal characteristics.

Available for download at
https://journals.biologists.com/dev/article-lookup/doi/10.1242/dev.202614#supplementary-data

Table S4. List of primers used for RT-qPCR experiments in zebrafish.

Gene	Forward 5'-3'	Reverse 5'-3'
tgfb1a	*TCCCGGATTCCTTGCTTTCG*	*ACTCCGCGATACAGTTCCAG*
tgfb2	*CTGCACATTTGTGCCGTCAA*	*AAGTCGATGTAGAGCGAGCG*
tgfb3	*CGGGCAGGACAACACTGA*	*GGCAGTAGGGCAGGTCATTG*
tgfbr1a	*GACCACCCATTCCTTGCTGA*	*TAGCAGAGGCAAACCTGAGC*
tgfbr2	*GGCTGATCACAGCGTTTCAC*	*CGACAGCGAGTTGTCCAAAC*
18s	GCTTTGCAACCATACTCCCC	CGGAGGTTCGAAGACGATCA

Available for download at
https://journals.biologists.com/dev/article-lookup/doi/10.1242/dev.202614#supplementary-data

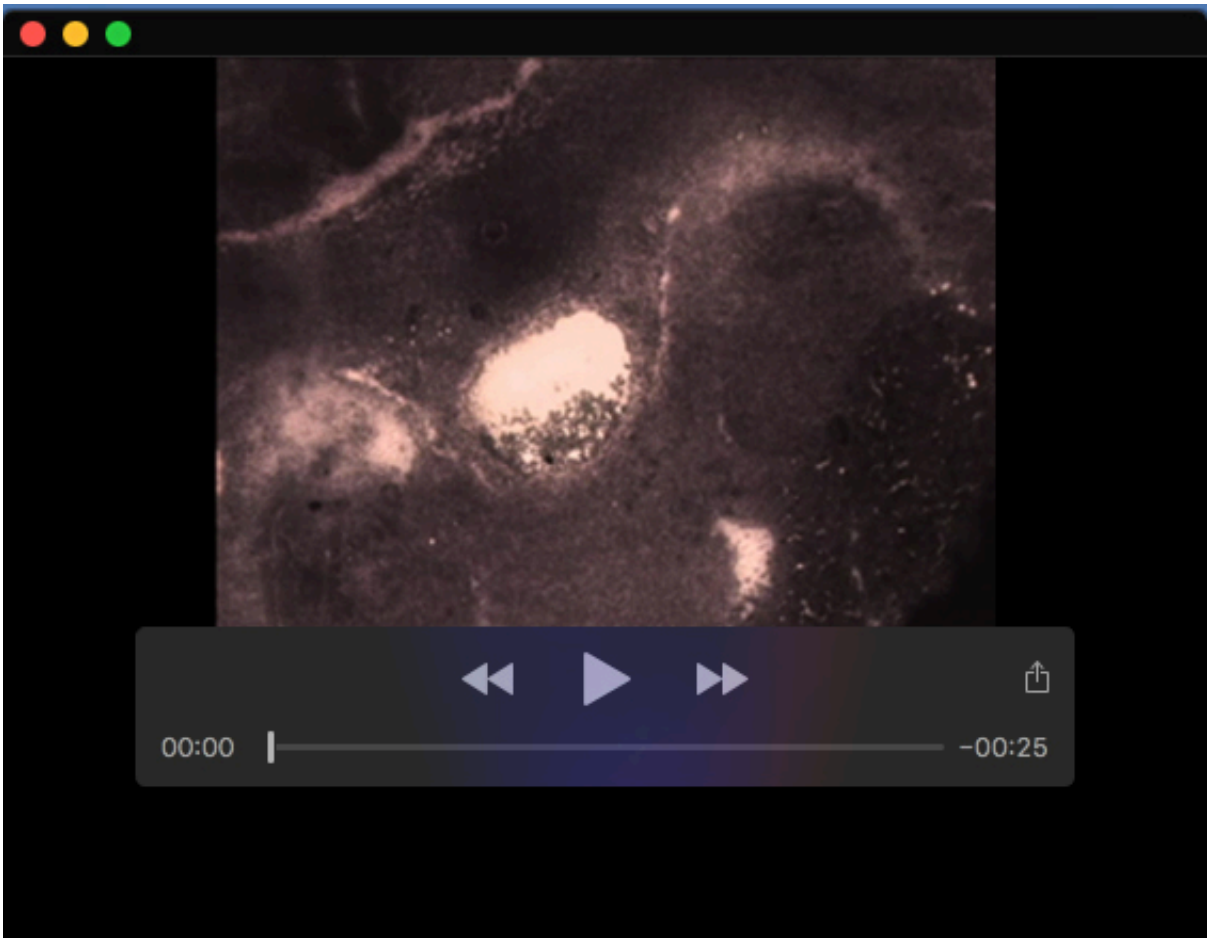

Movie 1. Laser microdissection. This movie illustrates the microdissection of the dorsal tissue located between the notochord and the roof of the dorsal aorta at E12.5. The green line indicates the trajectory of the ultraviolet laser used for cutting the tissue. The green spots indicate the position of the infrared laser used for capturing the microdissected tissue.

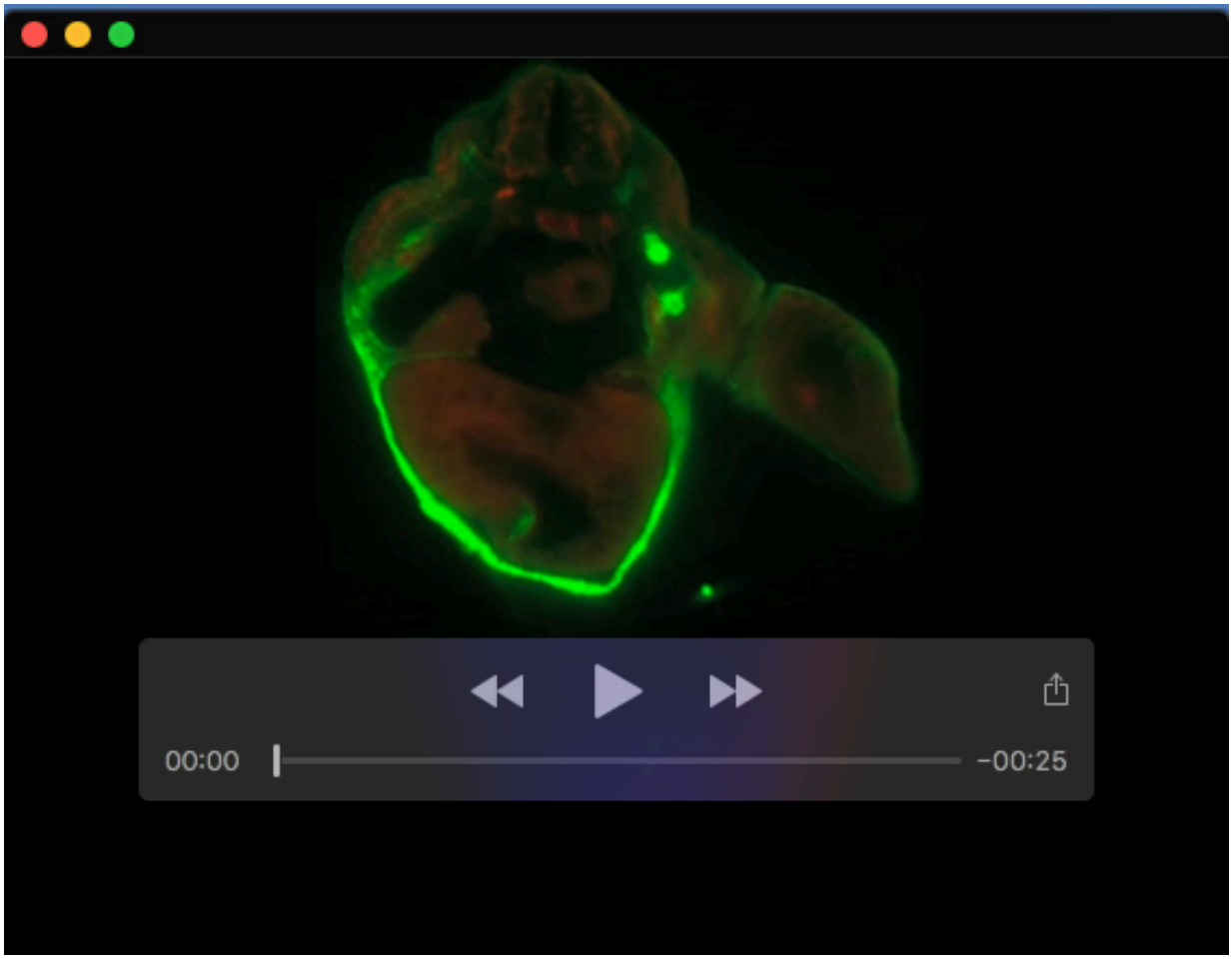

Movie 2. 3D imaging of Tnc (in green) and CD31 (in red) expression at E11.5. This video was generated using Arivis software after whole-mount immunostaining, 3DISCO clearing and imaging using an ultramicroscope (LaVision Bio Tec). The movie shows the expression profiling of Tnc and CD31 along the antero-posterior axis of the embryo.

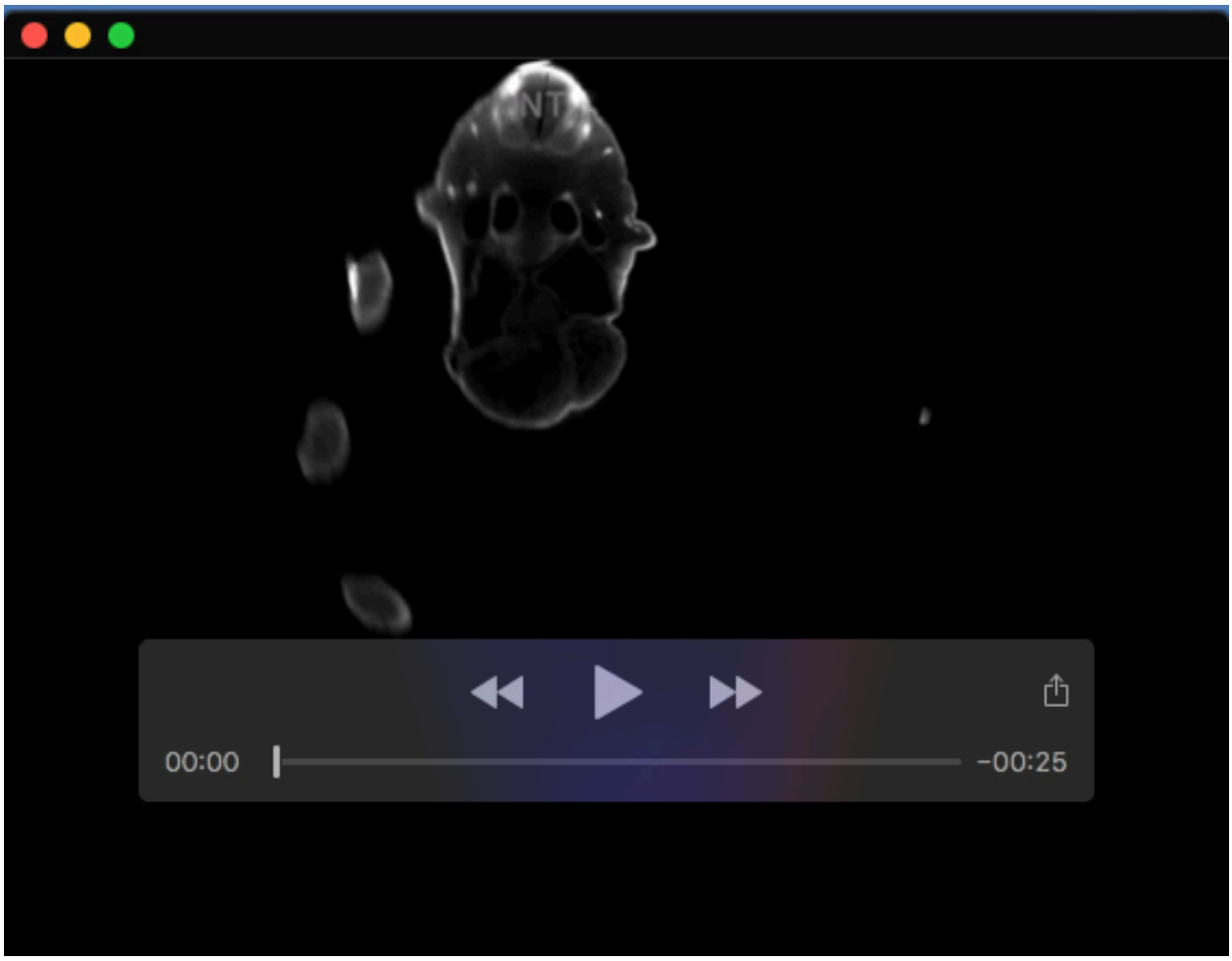

Movie 3. 3D analysis of Ntrk3 expression at E11.5. This video was generated as described above. The movie shows the expression profiling of Ntrk3 along the antero-posterior axis of the embryo.